NeuroImage: Clinical 17 (2018) 704–716

Contents lists available at ScienceDirect

NeuroImage: Clinical

journal homepage: www.elsevier.com/locate/ynicl

Altered intrinsic and extrinsic connectivity in schizophrenia

Yuan Zhou[a,b,c,d,*,1], Peter Zeidman[d,1], Shihao Wu[e], Adeel Razi[d,f], Cheng Chen[e], Liuqing Yang[a,c], Jilin Zou[e], Gaohua Wang[e], Huiling Wang[e,g,**], Karl J. Friston[d]

[a] CAS Key Laboratory of Behavioral Science, Institute of Psychology, Beijing 100101, China
[b] Magnetic Resonance Imaging Research Center, Institute of Psychology, Chinese Academy of Sciences, Beijing 100101,China
[c] Department of Psychology, University of Chinese Academy of Sciences, Beijing 100049, China
[d] The Wellcome Trust Centre for Neuroimaging, University College London, Queen Square, London WC1N 3BG, UK
[e] Department of Psychiatry, Renmin Hospital of Wuhan University, Wuhan 430060, China
[f] Department of Electronic Engineering, NED University of Engineering and Technology, Karachi, Pakistan
[g] Hubei Provincial Key Laboratory of Developmentally Originated Disease, Wuhan 430071, China

ARTICLE INFO

Keywords:
Dynamic causal modeling
Effective connectivity
Functional dysconnectivity
Schizophrenia
Working memory

ABSTRACT

Schizophrenia is a disorder characterized by functional dysconnectivity among distributed brain regions. However, it is unclear how causal influences among large-scale brain networks are disrupted in schizophrenia. In this study, we used dynamic causal modeling (DCM) to assess the hypothesis that there is aberrant directed (effective) connectivity within and between three key large-scale brain networks (the dorsal attention network, the salience network and the default mode network) in schizophrenia during a working memory task. Functional MRI data during an n-back task from 40 patients with schizophrenia and 62 healthy controls were analyzed. Using hierarchical modeling of between-subject effects in DCM with Parametric Empirical Bayes, we found that intrinsic (within-region) and extrinsic (between-region) effective connectivity involving prefrontal regions were abnormal in schizophrenia. Specifically, in patients (i) inhibitory self-connections in prefrontal regions of the dorsal attention network were decreased across task conditions; (ii) extrinsic connectivity between regions of the default mode network was increased; specifically, from posterior cingulate cortex to the medial prefrontal cortex; (iii) between-network extrinsic connections involving the prefrontal cortex were altered; (iv) connections within networks and between networks were correlated with the severity of clinical symptoms and impaired cognition beyond working memory. In short, this study revealed the predominance of reduced synaptic efficacy of prefrontal efferents and afferents in the pathophysiology of schizophrenia.

1. Introduction

Schizophrenia is a severe mental illness, with a variety of positive and negative clinical symptoms and cognitive impairments. The dysconnection hypothesis frames schizophrenia as a brain disorder, characterized by abnormal functional integration among brain regions (Andreasen et al., 1998; Bullmore et al., 1997; Friston et al., 2016; Friston and Frith, 1995; Stephan et al., 2006; Weinberger, 1993). Increasing evidence from functional connectivity studies, which examine correlations between fMRI timeseries across the brain, suggests that this dysconnection involves changes in coupling between large-scale brain networks (Fornito and Bullmore, 2015; Jiang et al., 2013; Pettersson-Yeo et al., 2011). However, functional connectivity methods do not reveal the causal influence of one neural system on another (Friston, 2011) and it remains unclear how the causal influences within and between large-scale brain networks are disturbed in schizophrenia.

Several studies have performed effective connectivity analyses to address this question (Crossley et al., 2009; Deserno et al., 2012; Nielsen et al., 2017; Schmidt et al., 2013; Schmidt et al., 2014; Zhang et al., 2013). Effective connectivity is the directed (causal) influence of one neural system over another, which is inferred by modeling the neuronal interactions that give rise to fMRI time series (Breakspear, 2004; Friston et al., 1993). Dynamic causal modeling (DCM) (Friston et al., 2003) is a widely adopted framework for effective connectivity analysis. Traditionally, DCM has been used to test competing hypotheses about brain networks comprising only a few regions (usually < 6) and directed connections. These hypotheses are specified in the form of subgraphs or models, which are subsequently

* Correspondence to: Y. Zhou, Institute of Psychology, Chinese Academy of Sciences, Beijing 100101, China.
** Correspondence to: H. Wang, Department of Psychiatry, Renmin Hospital of Wuhan University, 238 Jiefang Road, Wuhan 430060, China.
E-mail addresses: zhouyuan@psych.ac.cn (Y. Zhou), hlwang@whu.edu.cn (H. Wang).
[1] Equal contribution to this work as the first authors.

https://doi.org/10.1016/j.nicl.2017.12.006
Received 28 June 2017; Received in revised form 25 September 2017; Accepted 3 December 2017
Available online 05 December 2017

compared using Bayesian model selection and averaging. Following this approach, several studies have found abnormalities in effective connectivity in the fronto-temporal network (Crossley et al., 2009), the fronto-parietal network (Deserno et al., 2012; Nielsen et al., 2017; Schmidt et al., 2013; Schmidt et al., 2014) and the default mode network (Zhang et al., 2013) during working memory tasks in schizophrenia or psychosis. However, each of these studies focused on examining connectivity between regions *within* a single brain network and did not examine the connectivity *between* large-scale networks that contextualize functional integration in the brain.

In this study we investigated the effective connectivity within and between three key large-scale networks during a working memory task in schizophrenia. Working memory impairment is a common cognitive deficit in schizophrenia (Forbes et al., 2009; Lee and Park, 2005; Piskulic et al., 2007) and is considered to be a fundamental impairment that underwrites schizophrenic thought disorder (Goldman-Rakic, 1994). Multiple brain regions including lateral prefrontal cortices, posterior parietal cortices, insula and supplementary motor cortex extending to the anterior cingulate cortex (SMA/ACC) show co-activation during working memory tasks (Chu et al., 2015; Owen et al., 2005; Rottschy et al., 2012). These are commonly segregated into two key large-scale networks: the frontoparietal dorsal attention network (DAN) (Corbetta and Shulman, 2002; Fox et al., 2006) and the cingulate-opercular salience network (SN) (Dosenbach et al., 2007; Menon and Uddin, 2010; Seeley et al., 2007). Meanwhile, medial prefrontal and medial parietal regions often show deactivation during working memory tasks – these are part of the default-mode network (DMN) (Andrews-Hanna et al., 2010; Buckner et al., 2008; Raichle, 2015). In patients with schizophrenia, regions in the DAN and SN often show decreased activation (Anticevic et al., 2013; Kim et al., 2010; Kyriakopoulos et al., 2012), while the regions within the DMN often fail to deactivate during working memory tasks (Anticevic et al., 2013; Haatveit et al., 2016; Whitfield-Gabrieli et al., 2009). By including regions of the DAN, SN and DMN in a single connectivity model, we set out to investigate how the coupling between these networks is disturbed in schizophrenia.

A further novel feature of this study is that we apply recent developments in hierarchical Bayesian modeling, to make inferences based on a relatively large dataset (n = 102). In the Parametric Empirical Bayes (PEB) framework for DCM (Friston et al., 2016), an individual subject's connections are modeled as being sampled from a group mean, with additive random effects and systematic intersubject variability modeled by between-subject covariates. This hierarchical modeling of random parametric effects offers several advantages over previous methods. In particular, the uncertainty (variance) of estimated connection strengths at the single-subject level is properly accommodated when making inferences at the group level. This increases the sensitivity of the approach and renders it robust to outlier subjects with noisy data (Friston et al., 2016).

In this study, we used DCM – in conjunction with hierarchical modeling – to ask whether patients with schizophrenia show abnormalities in intrinsic (within-region) connectivity and extrinsic (between-region) connectivity in three large-scale brain networks (DAN, SM, DCM) while performing a working memory task. We further asked whether working memory load modulates this connectivity. Finally, we asked whether any abnormal directed connections are related to symptom severity and wider cognitive function to establish the functional validity of the effective connectivity estimates – that might be used a biomarker or endophenotype in subsequent studies.

2. Materials and methods

2.1. Participants

Patients with schizophrenia were recruited from the Department of Psychiatry, Renmin Hospital of Wuhan University (Wuhan, China). The Structured Clinical Interview for the Diagnostic and Statistical Manual of Mental Disorder, 4th edition (DSM-IV) (SCID) was administered, to confirm diagnosis. The patients also met the following inclusion criteria: (1) the total score of Positive and Negative Syndrome Scale (PANSS) was over 60, (2) duration of illness was < 5 years, (3) 18–45 years of age, (4) at least 9 years of education, (5) right-handed, and (6) Han Chinese. Patients were excluded if they met the diagnosis criteria of any other DSM Axis-I disorders, had severe physical illness including cardiovascular disease, had received electroconvulsive therapy six months prior to recruitment, or had structural changes in the brain (such as a white matter lesion) diagnosed by a radiologist. Healthy controls were recruited by word of mouth and bulletin board postings both in the hospital and nearby communities. The healthy controls, who matched the patients on age, gender and educational level, had the same inclusion and exclusion criteria; except that healthy controls were excluded if they or their first-relatives met any diagnosis of a psychiatric disorder according to the DSM-IV criteria.

Fifty-one patients and 66 healthy controls were recruited. All the patients were receiving antipsychotic medications, which were converted to their chlorpromazine equivalents. Six patients and 4 healthy controls were excluded from the data analyses due to severe head motion during scanning (x,y,z translation > 3 mm or x,y,z rotation > 3°), 3 patients were excluded due to extremely high values in the mean frame displacement (FD) value and 2 patients were excluded due to extreme low scores in the 0-back performance (see details in Methodology). Finally, 40 patients and 62 normal controls were included in the following data analyses.

Each participant or at least one first-degree relative for each patient provided informed consent before participation. The Ethics Committee of Renmin Hospital of Wuhan University and the Institutional Review Board of the Institute of Psychology, Chinese Academy of Sciences approved the study.

2.2. Experimental design and task

The WM paradigm used a blocked design, numeric n-back task, with numbers 0–9 as stimuli, which has been used in previous studies (Deserno et al., 2012; Salomon et al., 2011; Wu et al., 2017). The paradigm alternated between rest and task. Rest periods, in which subjects were instructed to fixate on a cross at the centre of the screen, lasted for 5 scans (i.e. 10 s). The task consisted of two conditions, 0-back (baseline) and 2-back (WM load condition), arranged as 0-2-0-0-2-2-2-0-0-2-2-0, each with duration of 12 scans (i.e. 24 s). Before each block a visual cue of one scan (i.e. 2 s) was presented, indicating the condition of the subsequent block. Each block comprised 12 stimuli, three of which were targets, each presented for 1000 ms with a 1000 ms interstimulus interval. Subjects were instructed to match the current number to a target, either the number 9 (0-back) or the number presented two trials earlier (2-back).

In order to ensure compliance during the subsequent acquisition, a training session was conducted prior to scanning. The training procedure was the same as that used in our previous study (Wu et al., 2017). In brief, the training task was similar to the formal task, though only one 0-back and one 2-back trial were included. Accuracy was displayed on the monitor at the end of the practice task, and patients were provided with further practice opportunities, until they clearly understood the task.

2.3. Cognition assessments

Several cognitive assessments were conducted outside of scanning. These included the Digit Symbol Coding task, Digit Span (forward and backward) and Category Fluency test. The Digit Symbol Coding task assesses information processing speed and is known to detect impairments in schizophrenia reliably (Bora et al., 2010). The Category Fluency test is the cognitive assessment with the second largest effect size,

followed by the Digit Symbol Coding task (Knowles et al., 2010). The Digit Span (forward and backward) is a general assessment of attention and working memory capacity.

2.4. MRI data acquisition and preprocessing

MRI data were acquired from the Radiology Department of Renmin Hospital of Wuhan University with a General Electric HDxt 3.0T Scanner. Whole-brain functional scans were collected in 32 axial slices using an echo-planar imaging (EPI) sequence (repetition time = 2000 ms, echo time = 30 ms; flip angle = 90°; matrix = 64 × 64; field of view = 220 mm × 220 mm; slice thickness = 4 mm; and slice gap = 0.6 mm). Anatomical images were acquired using a high-resolution T1-weighted sequence (repetition time = 7.8 ms; echo time = 3.0 ms; flip angle = 7°; matrix = 256 × 256; field of view = 256 × 256 mm^2; slice thickness = 1 mm) composed of 188 slices in a sagittal orientation.

Initial image preprocessing was performed using Statistical Parametric Mapping (SPM12) (http://www.fil.ion.ucl.ac.uk/spm/) and included slice timing correction, motion correction, structural and functional image co-registration, segmentation, normalization (based on each participant's structural image) to the Montreal Neurological Institute (MNI) 152 template, and smoothing using a kernel with a full-width half maximum of 6 mm. The normalized images were interpolated to a resolution of 3 × 3 × 3 mm^3. Furthermore, based on the head motion parameters obtained after realignment, we computed the volume-based frame-wise displacement (FD) to quantify head motion (Power et al., 2012; Satterthwaite et al., 2012; Van Dijk et al., 2012).

2.5. Behavioral analysis

To assess behavioral performance of the n-back task, the sensitivity index, d′ from signal detection theory was used. The score d′ describes sensitivity; i.e., the ability to separate signal (“true” events) and noise (“false” events) (Stanislaw and Todorov, 1999). The score was computed separately for 0-back condition and 2-back condition (d′0 and d′2) for each participant. A repeated measures ANOVA with conditions as within-group factor and diagnosis as between-group factor was conducted using SPSS 20.0. Two sample *t*-tests were used to assess group differences in the Digit Symbol Coding task, Digit Span task and Category Fluency task.

2.6. GLM analysis

A general linear model (GLM) was constructed with regressors for each of the two task conditions (0-back and 2-back) as well as the instruction cues for the task blocks. To regress out motion and physiological noise (e.g., of cardiac and respiratory origin), additional covariates were included to model: (1) six head motion parameters obtained by rigid body head motion correction and (2) five principal components from an anatomically defined noise VOI (composed of white matter and cerebrospinal fluid), an approach that has been shown to accurately describe physiological noise in grey matter (Behzadi et al., 2007). Finally, a highpass filter with a cutoff of 250 s (0.004 Hz) was implemented to remove low frequency drifts while retaining most task-related frequencies.

At the group level, random-effects group analyses were conducted using an ANOVA, with diagnosis as a between-group factor and task condition as a within-group factor. If not mentioned otherwise, significant effects in fMRI analyses were defined by a corrected voxel-level family-wise error (FWE) threshold of $p < 0.05$.

2.7. Dynamic causal modeling

2.7.1. VOI selections

Regions that showed differential activation between the patients and control groups in the context of WM (i.e., a significant interaction between diagnosis and task) or activation/deactivation in association with the task (i.e., a significant main effect of task) were considered as volumes of interest (VOI) for use in subsequent DCM analysis. Furthermore, in order to focus on the three networks of interest, i.e., dorsal attention network (DAN), salience network (SN), and default-mode network (DMN), preexisting templates were used as masks to identify peak voxels in the core regions in each of the three networks (Shirer et al., 2012). This procedure defined four nodes for the DAN: the bilateral frontal eye field (FEF) and the bilateral superior parietal lobule (SPL); three nodes for the SN: the SMA/ACC, the left anterior insula (AI) and the right AI; two nodes for the DMN: the medial prefrontal cortex (MPFC) and the posterior cingulate cortex (PCC). The group-level VOI locations are listed in Table 2. These were obtained by intersecting functional defined templates (Shirer et al., 2012) with regions showing a significant interaction between diagnosis and task or main effect of task at a lesser conservative threshold of cluster-level FWE $p < 0.05$ (cluster-defining threshold $p = 0.001$). We then searched for the local maximum within the group-level VOI and summarized the regional response with the first eigenvariate of (confound-corrected) voxels within a 6 mm radius. For the participants in which no supra-threshold voxels were identified, the first eigenvariate was extracted from a 6 mm sphere centered at the group-level maximum.

2.7.2. Individual level DCM specification and inversion

DCM is a framework for specifying, estimating and comparing generative models of imaging time series. Here we used the basic (deterministic) model for fMRI, in which a vector $z \in \mathbb{R}^n$ represents mass neural activity of each brain region at a given time. The derivative of z with respect to time $\dot{z}$ can be written as:

$$\dot{z} = f(z, u, \theta^n)$$

where u is the experimental input and θ^n are neuronal coupling parameters that determine the strength of connections within and between brain regions. This function is approximated using:

$$\dot{z} = (A + \Sigma_j u_j B^{(j)})z + Cu$$

where parameter matrix $A \in \mathbb{R}^{n \times n}$ represents the connectivity within and between each of the n regions (which in this study is the average connectivity of 0-back and 2-back conditions), $B^{(j)} \in \mathbb{R}^{n \times n}$ is the modulatory effect of experimental manipulation j on each connection and $C \in \mathbb{R}^{n \times J}$ is the direct driving influence of each of the J experimental conditions on each region. The predicted neuronal activity enters a haemodynamic model that incorporates a model of neurovascular coupling and the subsequent BOLD response. This provides the predicted fMRI time series that one would expect to measure, given the connectivity parameters $\theta^n = (A, B, C)$.

We specified a DCM for each participant. Model specification involved setting prior variances on the parameters in matrices A, B and C, where a prior variance of zero ‘switches off’ a connection and a non-zero prior variance ‘switches on’ a connection – so that it can be informed by data. Here, there were two experimental inputs ($J = 2$): the main effect of task (all 0-back and 2-back events) and working memory load (contrasting 0-back with 2-back). Task entered the model as a driving input (by setting the appropriate priors in matrix C). Working memory load entered the model as a modulatory input on each region's self-connection (i.e., intrinsic connection) by setting the appropriate priors on matrix B. The self-connections regulate a region's response to its inputs; i.e., they provide gain control in the model, akin to inhibitory inter-neurons – and consequent excitation-inhibition balance – in the brain. Thus, we modeled working memory load as modifying the sensitivity of each region to input from the rest of the network.

Each subject's model was inverted, providing estimates of the connection strength parameters $\theta^{(n)}$ which best explained the observed data. The resulting posterior densities were normally distributed, with expected values and covariance (uncertainty). Model estimation

additionally provided the free energy approximation to log model evidence F, which scores the quality of each model in terms of accuracy and complexity:

$$F \cong \log p(y \mid m) = \text{accuracy} - \text{complexity}$$

where y is the data and m is the model. One uses the free energy F to compare competing models, in order to find the least complex model of the data that accurately explains the most variance.

2.7.3. Empirical Bayes for group DCM

Having fitted each subject's DCM to their data, we next performed a second level analysis to estimate the group mean and the effect of diagnosis for each connection. This used recently developed routines for modeling connectivity at the group level (Parametric Empirical Bayes) in the context of DCM (Friston et al., 2016). Parametric Empirical Bayes (PEB) is a between-subject hierarchical or empirical Bayesian model over parameters that models how individual (within-subject) connections relate to group or condition means. This hierarchical approach treats each connection as a random (between-subject) effect, which is modeled by adding a random Gaussian variation to subject-specific predictions, based upon the group mean connectivity as well as between-subject effects such as diagnosis or age. This parametric random effects modeling is important because, unlike a classical test (e.g. *t*-test), it uses the full posterior density over the parameters from each subject's DCM – both the expected strength of each connection and the associated uncertainty (i.e. posterior covariance) – to inform the group-level result (i.e., group differences).

A PEB model has the following form:

$$\theta^{(2)} = \eta + \epsilon^{(3)}$$

$$\theta^{(1)} = \Gamma^{(2)}(\theta^{(2)}) + \epsilon^{(2)}$$

$$y_i = \Gamma_i^{(1)}(\theta^{(1)}) + \epsilon_i^{(1)}$$

Starting with the last line, the observed fMRI data y_i for subject i is generated by function $\Gamma_i^{(1)}$, which here is the subject's DCM, with parameters $\theta^{(1)}$ and observation noise $\epsilon_i^{(1)}$. The contribution of the PEB framework is that the DCM parameters $\theta^{(1)}$ are themselves represented by a group or second-level model, written on the second line of the equation. The second level function $\Gamma^{(2)}$ has parameters (e.g., average connection strengths) $\theta^{(2)}$, plus between-subject variability $\epsilon^{(2)}$. Finally, these second level parameters have priors, with mean η, as specified on the first line of the equation.

In this study, the first (within-subject) level of the model is the standard deterministic DCM for fMRI, where the parameters correspond to effective connectivity (please see above). The second (between-subject) level model $\Gamma^{(2)}$ is simply a GLM with the form:

$$\Gamma^{(2)}(\theta^{(2)}) = (X \otimes I_P)\beta$$

where $X \in \mathbb{R}^{S \times C}$ is the design matrix (S is the number of subjects, C is the number of covariates), I_P is the identity matrix of dimension P (where P is the number of connection parameters in the DCM) and the operator $\otimes$ is the Kronecker product that duplicates each element of the design matrix for each DCM parameter. In other words, this model allows for every between subject-effect to be expressed at every within-subject effect. The parameters of the GLM are $\beta \subset \theta^{(2)}$. Thus, we had one β parameter representing the effect of each (between-subject) covariate on each DCM connection. The priors on these second level parameters were set to match the priors of the first level parameters. In order to identify differences between patients with schizophrenia and normal controls, we included two covariates of interest in the design matrix X: the group mean and diagnosis. We also included the working memory performance indexed by the ratio between d′2 score and d′0 score and the interaction between diagnosis and performance as nuisance covariates, in order to exclude the potential influence of performance components on the group mean and diagnosis effect.

The between-subject variability $\epsilon^{(2)}$ with precision $\Pi^{(2)}$ was parameterized using a single precision parameter γ:

$$\epsilon^{(2)} \sim N(0, \Sigma^{(2)})$$

$$\Pi^{(2)} = \Sigma^{(2)-1} = I_S \otimes (Q_0 + e^{-\gamma} Q_1)$$

where Q_0 is the lower bound on precision, which takes on a small positive value, and the precision parameter $\gamma \subset \theta^{(2)}$ scales a precision component Q_1. Here, we used the defaults in SPM, which sets Q_1 to $\left(\frac{1}{\beta} pC\right)^{-1}$, where pC is the prior covariance matrix of a single subject's DCM parameters and $\beta = 16$.

To summarize, the PEB model estimates the effect of each covariate on each connection (both the group mean and any group differences), as well as estimating the between-subject variability. The parameters of the PEB model were estimated using a standard variational Laplace procedure, as is usually applied in DCM.

2.7.4. Bayesian model reduction

To evaluate how the connectivity of patients with schizophrenia differs from that of normal controls, we used Bayesian model comparison to explore the space of possible hypotheses (models), where each hypothesis or model assumes that a different combination of the connections could exist across participants or show phenotypic variance. Candidate PEB models were obtained by removing one or more (second level) parameters from the full PEB model (described above) to produce reduced forms of the full model that differed only in their priors. We did this using Bayesian model reduction (BMR) that enables the evidence and parameters of nested (reduced) models to be derived directly from a full model. This provides an efficient search of the model space by scoring each reduced model, based on its log model-evidence or free energy; for details, see (Friston et al., 2016). The (greedy) search algorithm used BMR to iteratively prune connection parameters from the full PEB model, until model-evidence started to decrease. The parameters of the best 256 pruned models were then averaged, weighted by their evidence (Bayesian Model Averaging).

To summarize the DCM analysis pipeline, we first specified a DCM for each subject and fitted it to their data, providing estimates of the connectivity parameters. These subject-specific estimates (expected values and covariance) were taken to the group level and modeled using a Bayesian GLM (i.e., a PEB model). The parameters of the GLM represent the group average of each connectivity parameter, as well as any group differences between patients and controls. We than used Bayesian model reduction to search over hundreds of reduced PEB models with different combinations of connections (and group differences). The best models from this search were combined using Bayesian model averaging. We report these averages in the Results section.

2.8. Clinical correlates of differentiated connections

Having identified the connections that differed between patients and controls in the working memory task, we next asked whether the strength of these connections correlated with the severity of symptoms in patients. As we had a large number of variables, we did not include these in the PEB model directly; instead, we used a (post hoc) canonical variates analysis (CVA; Sui et al., 2012) to identify linear relationships between the two sets of measures (strength of effective connectivity and clinical symptoms). This resulted in pairs of significantly correlated canonical variables (i.e., latent connectivity and symptom profiles). Using the same analysis, we asked whether our cognitive scores could be predicted by the effective connectivity.

2.9. Effect of antipsychotic medication

In order to ameliorate the confounding effect of antipsychotic medication on group differences, we included the chlorpromazine

Table 1
Demographic and clinical characteristics.

	Patients	Controls	*p* Value
	(*n* = 40)	(*n* = 62)	
Gender (male/female)	21/19	35/27	0.84[a]
Age (years)	23.40 ± 4.22	23.58 ± 4.90	0.85
Education (years)	12.98 ± 2.93	13.47 ± 1.59	0.33
mean FD (mm)	0.07 ± 0.03	0.06 ± 0.02	0.1
0-Back (d-prime score)	3.81 ± 0.46	4.08 ± 0.29	0.001
2-Back (d-prime score)	2.32 ± 0.90	3.26 ± 0.56	< 0.001
Digit symbol coding	52.08 ± 10.23	70.89 ± 10.14	< 0.001
Digit span: forward	7.93 ± 1.23	9.00 ± 0.99	< 0.001
Digit span: backward	4.58 ± 1.28	6.27 ± 1.42	< 0.001
Category fluency	18.05 ± 3.52	21.74 ± 4.35	< 0.001
PANSS			
Total	2.90 ± 10.23	–	–
Positive	22.55 ± 3.59	–	–
Negative	19.23 ± 5.20	–	–
General	41.13 ± 6.41	–	–
Chlorpromazine equivalents (mg/d)	414.10 ± 236.74	–	–
Duration (months)	26.28 ± 20.49	–	–

Note: mean FD, mean frame-wise displacement; PANSS, Positive and Negative Symptom Scale; [a], Chi-square test; −, no value.

Table 2
Locations of volumes of interests.

Regions	MNI coordinates			Effect	Network
	x	y	z		
L.FEF	− 33	0	57	Interaction	DAN
L.SPL	− 27	− 60	45	Interaction	DAN
R.FEF	30	3	57	Interaction	DAN
R.SPL	33	− 66	57	Interaction	DAN
L.SMA/ACC	− 9	12	63	Interaction	SN
L.AI	− 45	18	− 3	Interaction	SN
R.AI	33	21	0	Task	SN
MPFC	− 9	48	− 15	Interaction	DMN
PCC	− 6	− 48	27	Task	DMN

Abbreviation: AI, anterior insula; DAN, dorsal attention network; DMN, default mode network; FEF, frontal eyes field; MPFC, medial prefrontal cortex; PCC, posterior cingulate cortex; SMA/ACC, supplementary motor cortex extending to anterior cingulate cortex; SN, salience network; SPL, superior parietal cortex.

equivalents of antipsychotic medication as a nuisance covariate – in addition to the nuisance covariates above (working memory performance and interaction between diagnosis and performance) – in the between subject design matrix. The main effects of group were unchanged when including antipsychotic medication as a between subject effect. We present the effect of the antipsychotic medication and other nuisance covariates on effective connectivity in the supplementary materials (Fig. S1). We also include the chlorpromazine equivalents of antipsychotic medication into the CVA models while exploring the clinical correlates of differentiate connections.

3. Results

3.1. Behavioral results

There were no group differences in the age, gender composition, educational level and head motion (all $p > 0.05$, Table 1). Repeated measures ANOVA using d′ score with the task condition as the within-group factor and diagnosis as the between-group factor revealed a significant main effect of task ($F = 256.03$; $df = 1$; $p < 0.001$), significant main effect of diagnosis ($F = 46.74$; $df = 1$; $p < 0.001$) and a significant interaction effect between task and diagnosis ($F = 21.42$; $df = 1$; $p < 0.001$); with the patients showing worse performance in the 2-back condition compared to the normal controls (Table 1). Two-sample *t*-tests also indicated impaired cognitive functions measured by the Digit Symbol Coding task, Digit Span task and Category Fluency task in patients with schizophrenia (all $p < 0.001$) (Table 1).

3.2. Brain activation following GLM analysis

There was a significant main effect of task in the bilateral lateral prefrontal cortices, lateral posterior parietal cortices, the ACC, the AI, the MPFC and the PCC, the thalamus and cerebellum ($p < 0.05$, whole-brain voxel-wise FWE correction) across healthy controls and patients with schizophrenia (Fig. 1), showing that the regions comprising the DAN, the SN and the DMN were engaged by this task. No main effect of diagnosis was found ($p < 0.05$, whole-brain voxel-wise FWE correction). A significant task by diagnosis interaction was found in the left FEF, left inferior frontal gyrus, left SPL, ACC, left caudate and left precuneus ($p < 0.05$, whole-brain voxel-wise FWE correction) (Fig. 1). Using a more liberal statistical threshold, a task by diagnosis interaction could also be found in the MPFC and the left AI ($p < 0.05$, cluster level FWE correction). Fig. 2 shows the activation parameter estimates for each condition in the peak coordinates of the regions that were entered into the following DCM analyses.

3.3. Task independent connectivity across conditions – and their group differences

After specifying and estimating DCMs, we assembled the parameters from each subject's model (matrix *A*). These parameters represent the average connectivity over 0-back and 2-back conditions. We fitted a PEB model to the posterior density over these parameters to estimate the group mean of each connection strength, and the effect of diagnosis on each connection (see methods). Fig. 3 shows the group mean across all subjects. The left panel shows the parameter estimates before and after Bayesian model reduction, in terms of their posterior means (grey bars) and 95% confidence intervals (pink lines). It can be seen that some parameters were removed, because they were not necessary to explain the data. The right panel shows this reduced model as a schematic. Our main interest regarded differences between subjects, so we will just make one observation about this result: it is apparent that most regions had reciprocal excitatory influences on one another (green arrows), with the exception of the DMN (regions MPFC and PCC). Connections entering the DMN were generally inhibitory (red arrows), whereas outgoing connections from the DMN were generally excitatory. Thus, the model suggests that deactivation of the DMN during working memory tasks can be explained by inhibition of the DMN by the DAN and SN.

Fig. 4 shows group differences in connectivity. The left panel illustrates the corresponding parameter estimates from the PEB model before and after Bayesian model reduction. Only a restricted set of parameters survived model reduction, which is illustrated in the right hand panel. Specifically, the patients with schizophrenia had decreased inhibitory self-connections (intrinsic connections) within the DAN regions; in particular left FEF and the left SPL, where the differences were negative (parameters 1 and 11 in Fig. 4 and Supplementary Table 1). Note that these parameters are log scale parameters such that a negative difference corresponds to a smaller self-inhibition; namely, a relative disinhibition in patients. Thus, we could be confident that left FEF and left SPL were more readily excited by afferent activity in patients with schizophrenia than controls. There were also small differences in extrinsic connections, demonstrated by coupling among regions in the DAN (bilateral FEF and lSPL) and between regions of the DAN and the other networks. Patients had reduced coupling from lFEF to rFEF compared to controls (parameter 3 in Fig. 4 and Supplementary Table S1). However, we could not determine the sign of the other extrinsic (between-region) connections in the DAN, as their 95%

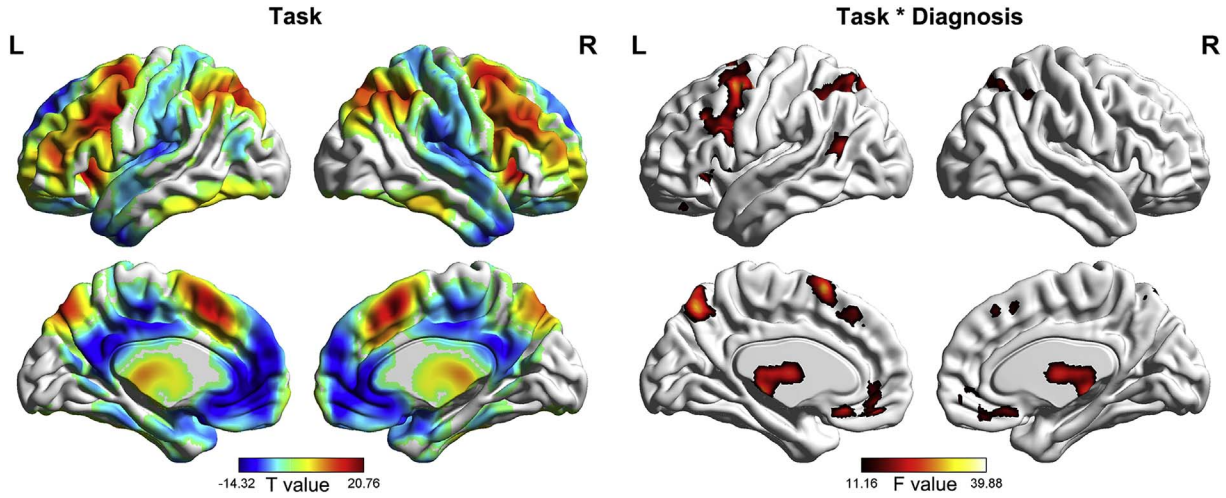

Fig. 1. Regions showing a significant main effect of task condition and regions showing a significant interaction effect (between diagnosis and task condition). Left: Colors indicate T-statistics. Warm colors represent greater activation in the 2-back condition and cool colors represent less activation (i.e., greater deactivation) in the 2-back compared with the 0-back condition. Right: Interaction contrast, where hotter colors indicate larger effects. Colors indicate F-statistics. Thresholded at $p < 0.05$ (cluster level FWE corrected) for visualization purposes. These regions were projected on a cortex using BrainNet Viewer (www.nitrc.org/projects/bnv/). (For interpretation of the references to color in this figure legend, the reader is referred to the web version of this article.)

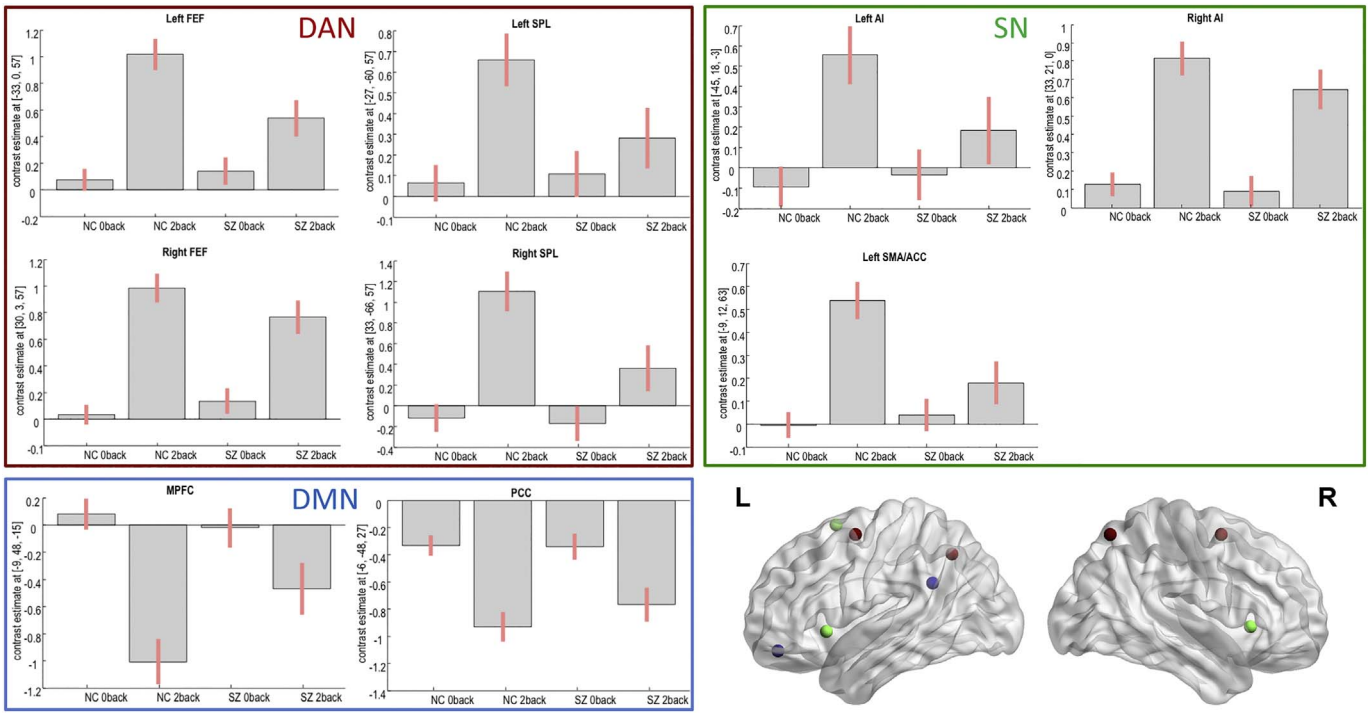

Fig. 2. Estimated activation contrast parameters for the peak coordinate of the volumes of interest (VOI) used in subsequent DCM. The grey bars represent the estimated effect size and the pink lines represent 90% confidence interval. In the right lower panel, the locations of VOIs are shown in the cortex using BrainNet Viewer (www.nitrc.org/projects/bnv/). Red balls represents the DAN regions, the green balls the SN regions and the blue balls if, the DMN regions. For abbreviations, please see Table 2. (For interpretation of the references to color in this figure legend, the reader is referred to the web version of this article.)

confidence intervals included zero (parameters 2, 19, 21, 23, 66 in Fig. 4 and Supplementary Table S1). Given that these small differences in extrinsic connections were not pruned during Bayesian Model Reduction, we could be confident that despite being small effects individually, they collectively contributed to the model evidence. Strikingly, we found that patients with schizophrenia had stronger extrinsic connectivity within the DMN, specifically in the direction from PCC to MPFC. This accords with the hypothesis that patients with schizophrenia fail to deactivate their DMN during externally directed tasks. For clarity, Fig. 5 plots the strength of the connections that showed between-groups effects.

3.4. Modulatory effects on connections and their group differences

Fig. 6 shows the group mean effect of WM load before and after model reduction. We found a strong effect of working memory load on the self-connections (intrinsic connections) of all the regions of the DAN (parameters 1–4) but on none of the remaining regions. These effects were negative, meaning that self-inhibition was reduced during higher working memory load (i.e. greater excitation with 2-back relative to 0-back conditions). We did not find any group differences in the modulatory effect of working memory load between patients and controls.

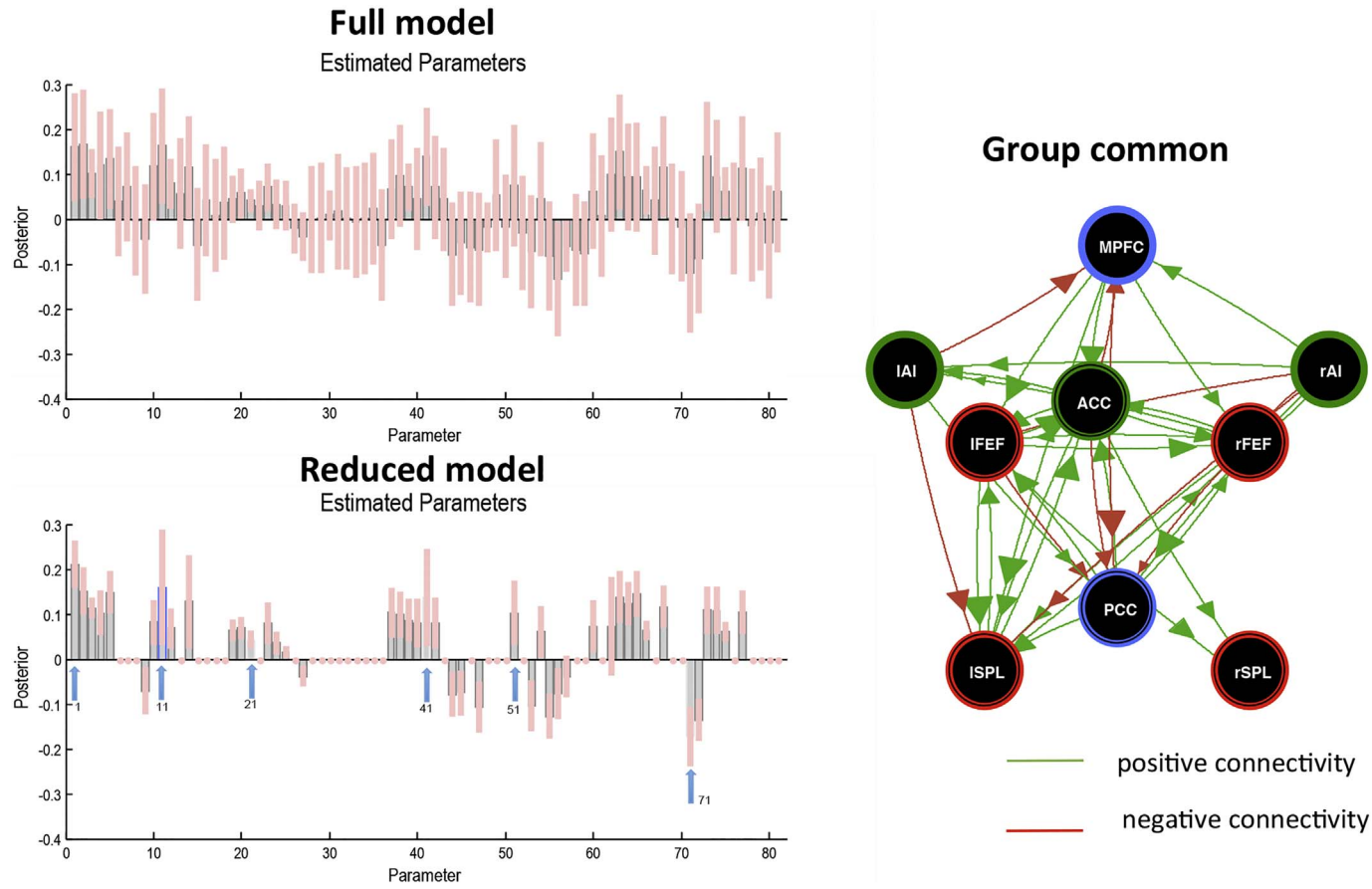

Fig. 3. The group mean effective connectivity (average of 0-back and 2-back conditions). The left panel shows the posterior estimates of the second level models before (Full model) and after Bayesian model reduction (Reduced model), in terms of their posterior means (grey bars) and 95% Bayesian confidence intervals (pink lines). The self-connections in the reduced model are indicated using the blue arrows. The parameters along the horizontal axis constitute the connections. For a list of these parameters, please see the Supplementary Table S1. The right panel shows the connections from the reduced model in a schematic. The green arrows represent the positive extrinsic effective connectivity and the red arrows represent the negative extrinsic effective connectivity. The size of the arrow reflects the relative strength of connectivity. For abbreviations of the region names, please see Table 2. (For interpretation of the references to color in this figure legend, the reader is referred to the web version of this article.)

3.5. Clinical correlates of differentiated connections

Returning to the connections showing group differences in effective connectivity, we performed a CVA analysis to ask whether the severity of clinical symptoms in schizophrenia could be predicted from the estimated connectivity. There was a significant canonical correlation (p = 0.04, Chi-square = 52.7, df = 36) (Supplementary Fig. S2, left panel) although this became insignificant after excluding the effects of age, gender, education level and dosage of antipsychotic medicine (p = 0.08, Chi-square = 48.5, df = 36). The connections that contributed the most to this relationship (had the largest absolute canonical weights) were the left FEF self-connection and the left SPL self-connection.

In addition, the connection strengths predicted impaired processing speed (digit symbol task), attention and working memory (digit span forward and backward task), and executive function (verbal fluency task) within the patient group (p = 0.04, Chi-square = 52.6, df = 36) (Supplementary Fig. S2, right panel), even after excluding the effects of age, gender, education level and dosage of antipsychotic medicine (p = 0.05, Chi-square = 51.3, df = 36). The connections that contributed the most to this association were the left FEF self-connection and the connections between left and right FEF. These same tests of cognitive function were also given to the control subjects, and the connection strengths could also predict the scores collapsed across groups (p = 0.05, Chi-square = 51.0, df = 36). This result suggests that the connectivity parameters identified using DCM capture variability in more general cognitive abilities than the specific WM task used during scanning.

4. Discussion

This study investigated the effective connectivity of three large-scale networks; i.e., the dorsal attention network, salience network and default-mode network, during a working memory task. By capitalizing on recent developments in the hierarchical modeling of effective connectivity, we identified parameters that reliably distinguished patients with schizophrenia from controls. Our main findings were: in patients (i) self-inhibition in regions of the dorsal attention network was decreased across task conditions, implicating disinhibition – and a failure of excitation-inhibition balance – in the pathophysiology of schizophrenia; (ii) the connection from the PCC to the MPFC was increased across task conditions, which extends our knowledge from correlations (functional connectivity) to directed connectivity; (iii) the between-network connections involving the prefrontal cortex were altered across task conditions; (iv) the connections that differentiated patients from controls correlated with the severity of clinical symptoms and impaired cognition beyond working memory, suggesting that the physiological changes in connectivity have a clinical and cognitive predictive validity.

4.1. Impaired self-inhibition in schizophrenia

We found that self-inhibition in the DAN regions (left FEF and the left SPL) was impaired across task conditions in patients with

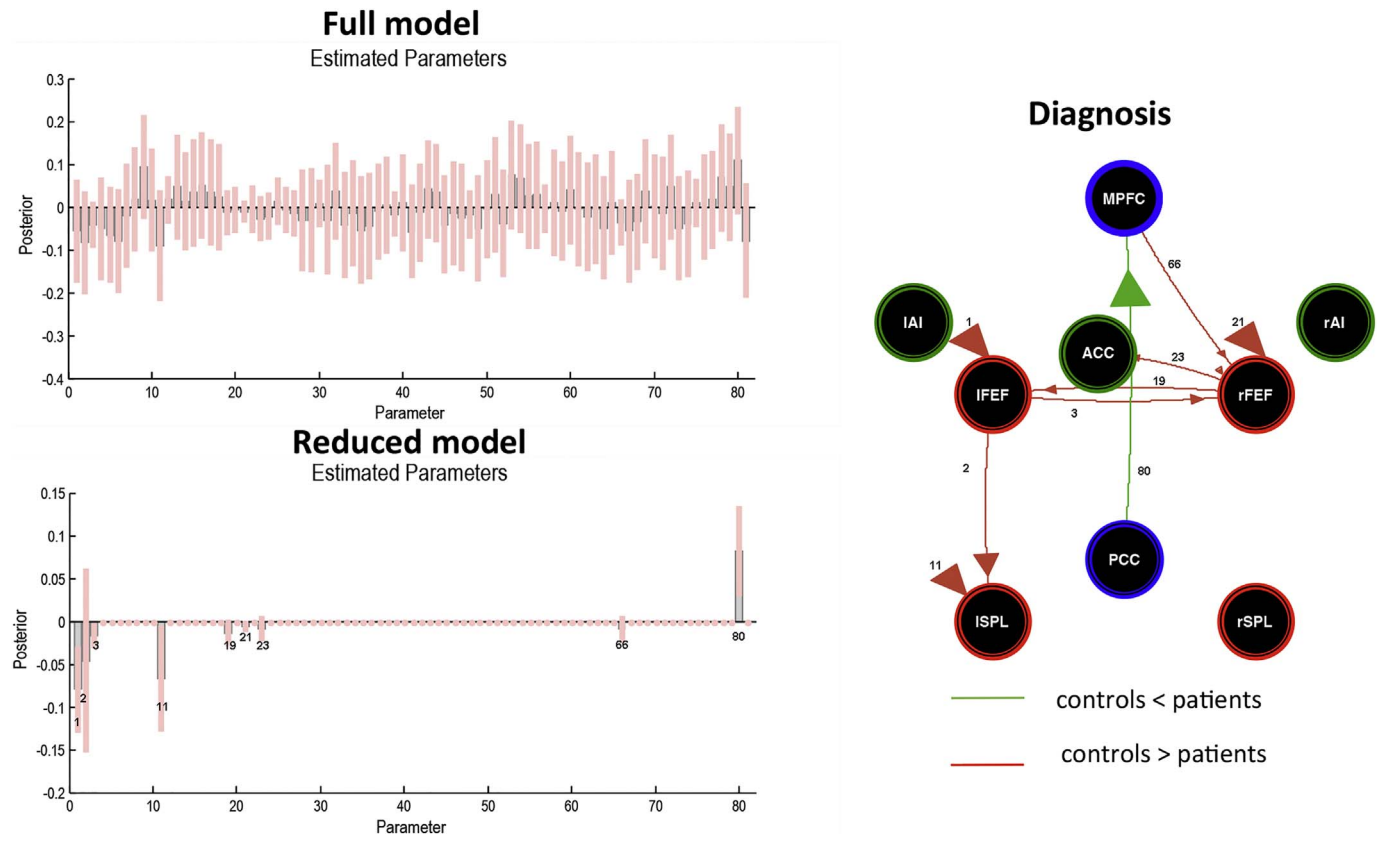

Fig. 4. The group difference (patients versus controls) of effective connectivity (average of 0-back and 2-back conditions). The left panel shows the posterior estimates of the second level models before (Full model) and after Bayesian model reduction (Reduced model), in terms of their posterior means (grey bars) and 95% Bayesian confidence intervals (pink lines). The parameters along the horizontal axis constitute the connections. For a list of these parameters, please see the Supplementary Table S1. The right panel shows connectivity differences with strong evidence in a schematic. The green line represents the increased effective connectivity in patients with schizophrenia and the red line represents the decreased effective connectivity. The differences in the self-connections are indicated by individual arrowheads directed at the relevant nodes. The size of arrow reflects the quantitative differences in connectivity. The connections showing salient effect are highlighted using their indices from the graph (and Table S1). Abbreviations for the region names are provided in Table 2. (For interpretation of the references to color in this figure legend, the reader is referred to the web version of this article.)

schizophrenia. From the perspective of predictive coding, these changes may reflect an aberrant precision or salience of prediction errors at the associated levels of the cortical hierarchy. To briefly reprise, in predictive coding, neuronal representations in higher levels of cortical hierarchies generate predictions of representations in lower levels. These top-down predictions are compared with representations at the lower level to form a prediction error (usually associated with the activity of superficial pyramidal cells). This mismatch signal is passed back up the hierarchy, to update higher representations (associated with the activity of deep pyramidal cells). This recursive exchange of signals suppresses prediction error at each and every level to provide a hierarchical explanation for sensory inputs (Bastos et al., 2012). Besides predicting the content of our sensations, the brain also has to predict the context in terms of expected or subjective precision. The brain may solve this generic problem by modulating the gain or excitability of neuronal populations reporting prediction errors (Clark, 2013; Friston et al., 2014). In the DCM framework, this gain is parameterized as the self-inhibition of superficial pyramidal cells within a cortical source (Ranlund et al., 2016). During the n-back task, the participant implicitly predicts whether the next stimulus is the same as the previously presented stimulus and a prediction error may emerge while comparing the current stimulus with the previously presented stimulus. In this context, the impaired self-connections in the dorsal attention network in patients with schizophrenia reflect a disinhibition in the superficial pyramidal cells in the constituent dorsal fronto-parietal regions. The disinhibition of the dorsal attention network in patients with schizophrenia may correspond to aberrant precision, which is thought to be encoded by the postsynaptic gain of neurons reporting prediction error (Adams et al., 2013). This aberrant precision or postsynaptic gain control may explain impaired working memory performance.

This disinhibition in schizophrenia is also in line with theories of *N*-methyl-D-aspartate receptor (NMDA-R) hypofunction in psychosis (Abi-Saab et al., 1998; Coyle et al., 2003; Gilmour et al., 2012; Olney et al., 1999; Stephan et al., 2006). The glutamatergic NMDA-R, which is expressed more densely in superficial cortical layers, is one of the predominant neurotransmitter receptors involved in gain modulation (Stephan et al., 2006). NMDA-R hypofunction on fast-spiking and parvalbumin-contained interneurons, which are gamma-aminobutyric acid (GABA)-ergic cells, is thought to lead to a failure in the regulation of the firing rate of pyramidal glutamatergic cells through inhibitory GABAergic input and thus causes an excitatory-inhibitory imbalance in prefrontal cortex (Carlen et al., 2012; Lewis et al., 2012; Ranlund et al., 2016). The cellular excitation–inhibitory imbalance may lead to disturbances in the neural synchrony of large-scale cell ensembles and give rise to dysconnectivity phenomena at the level of neural ensembles and large-scale brain networks in schizophrenia (Braun et al., 2016; Phillips and Silverstein, 2003; Uhlhaas and Singer, 2012). In the current study, we indeed noted decreased inter-regional connections involving regions showing disinhibition (in particular the connectivity between the left and right FEF). Furthermore, it should be noted that these changes were observed in the context of a working memory task, which is in line with the role of NMDA-R hypofunction in the cognitive impairments including attention allocation and working memory (Carlen et al., 2012; Monaco et al., 2015; Murray et al., 2014).

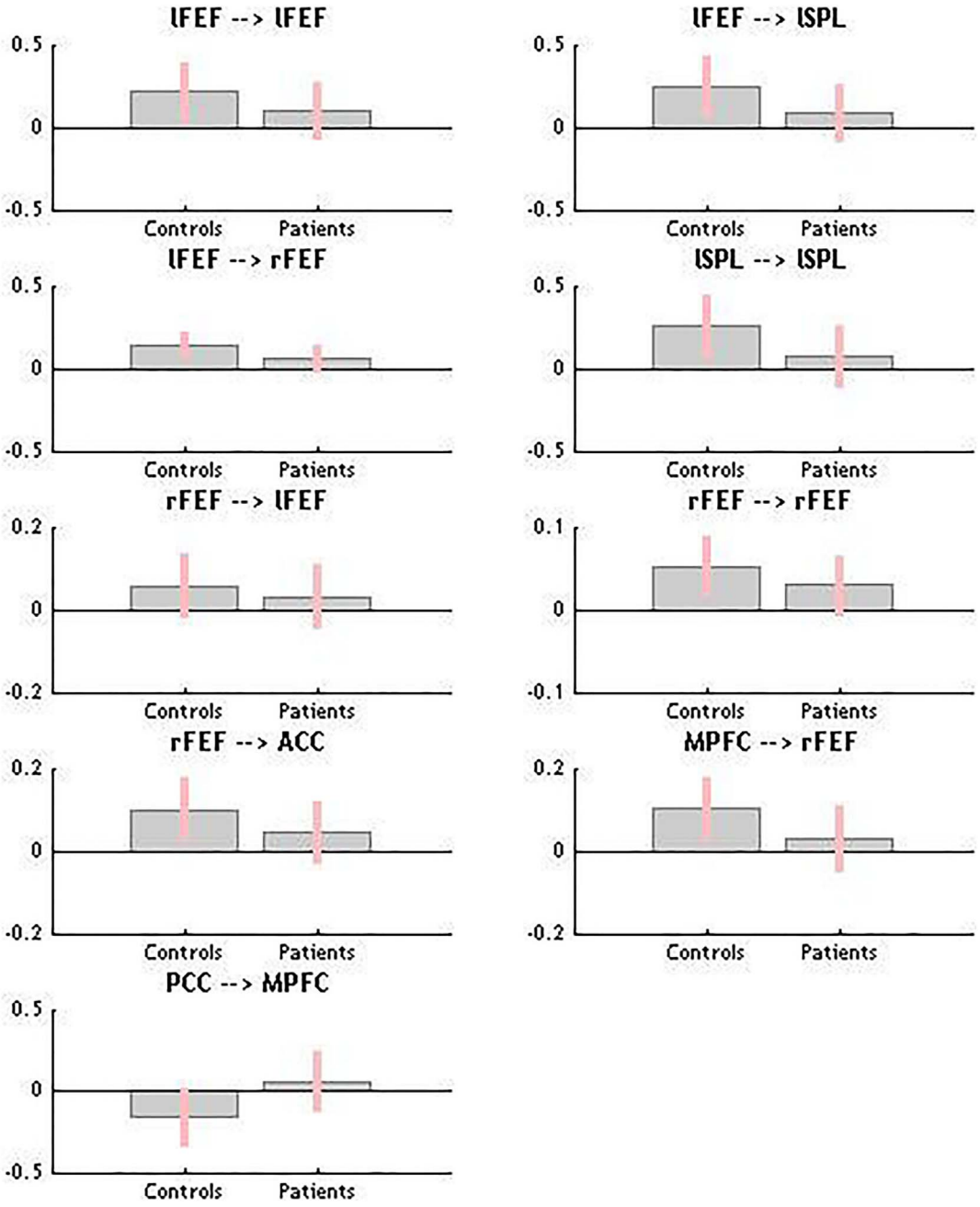

Fig. 5. Connections showing evidence for group differences. The vertical axis represents the connection strength. For self-connections, the parameters are log scaling parameters, which can be converted to units of Hz by: $y = -0.5 * \exp(x)$. Where x is the log scaling parameter, -0.5 Hz is the prior and y is the self-connection strength in units of Hz.

4.2. Altered effective connectivity within the DMN in schizophrenia

The connection from PCC to MPFC was greater in the schizophrenic subjects than the controls. This finding extends our prior knowledge by demonstrating that in addition to the altered functional connectivity within the DMN in schizophrenia (Whitfield-Gabrieli et al., 2009), the causal configuration of directed coupling between neural populations is altered. This finding is also similar to Wu et al.'s (2014) study but our finding was obtained from a larger DCM model that makes it possible to investigate the effective connectivity between regions from different brain networks. We also note a Granger causality study, in which directed functional connectivity from the PCC to the MPFC was increased during 2-back conditions in schizophrenia; however, the sign of the connectivity was not reported (Pu et al., 2016). With DCM, inferences about both the direction and valence (i.e., excitatory or inhibitory) of connections among neuronal sources (Friston et al., 2013), may extend our understanding of extrinsic connectivity within the DMN. Our results suggest that greater activity in the MPFC may come about due to decreased inhibitory influences from the PCC. Therefore, this finding provides a new explanation for the commonly observed hyperactivity in the MPFC (a failure of deactivation) in patients with schizophrenia (Whitfield-Gabrieli et al., 2009; Wu et al., 2014; Zhang et al., 2013).

This finding is also compatible with a recent observation, in which the reduced sensitivity to both extrinsic (excitatory) and intrinsic afferents in the MPFC during a picture-viewing task paradigm with a long rest period was found in schizophrenia (Bastos-Leite et al., 2015). A difference between their results and those of our current study is that our patients showed reduced sensitivity to the extrinsic (inhibitory) afferent to the MPFC during a working memory task. Although there are several methodological differences (such as the task paradigm, model

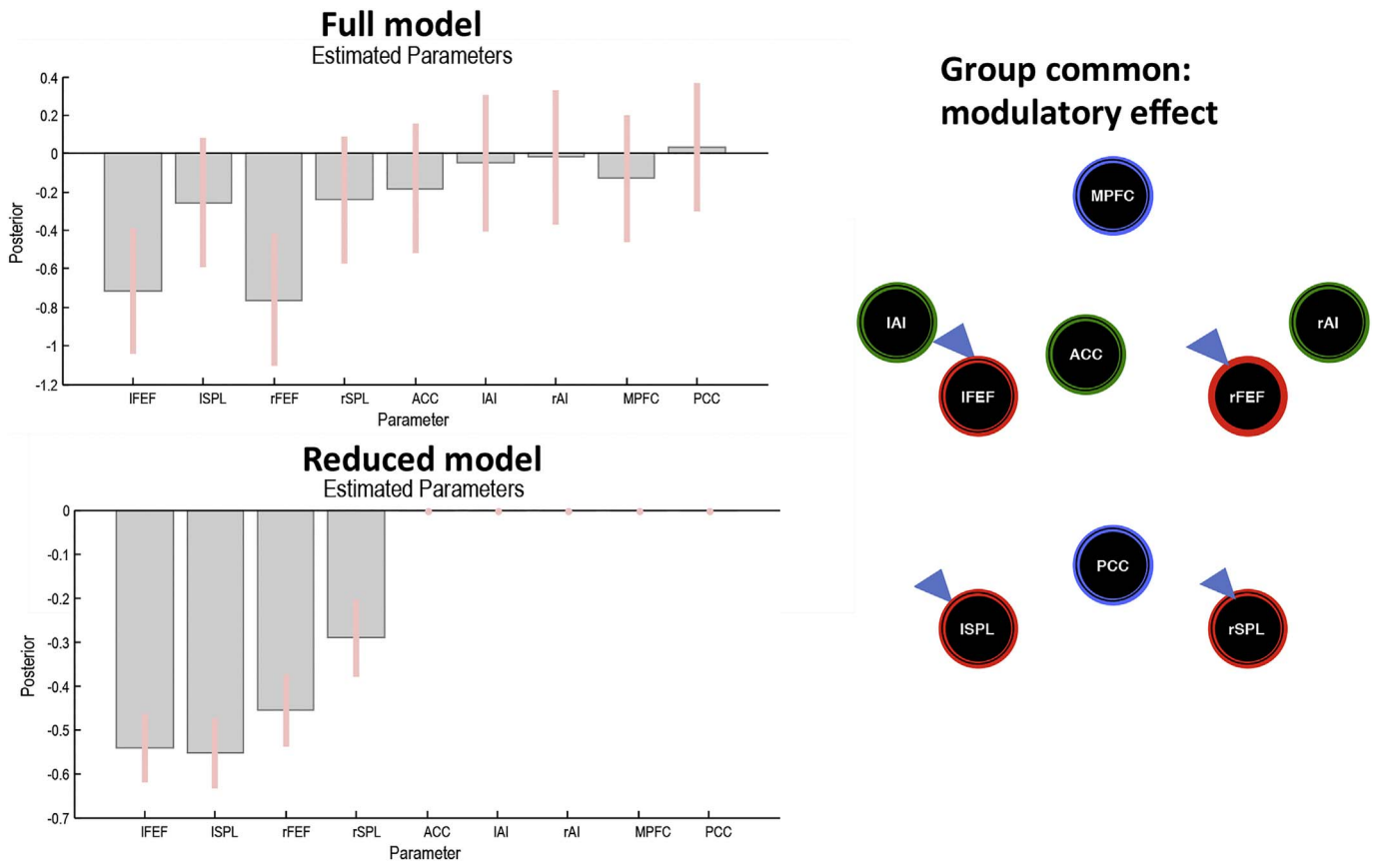

Fig. 6. The group mean effect of working memory load. This reflects the contextual modulation of (intrinsic regional) connectivity (i.e., matrix B in the DCM state equation). The left panel shows the posterior estimates of the second level models before (Full model) and after Bayesian model reduction (Reduced model), in terms of their posterior means (grey bars) and 95% Bayesian confidence intervals (pink lines). Only self-connections were included in this model. The right panel shows the connections with strong evidence in this reduced model as a schematic. Abbreviations for the region names are provided in Table 2. (For interpretation of the references to color in this figure legend, the reader is referred to the web version of this article.)

inversion and model space) between the two studies, both of these studies suggest that the medial prefrontal cortex fails to modulate its sensitivity to posterior parietal afferents. In the theoretical framework of the dysconnection hypothesis, the symptoms of schizophrenia are generally construed as false inferences (e.g., hallucinations and delusions), which reflect an aberrant encoding of salience or precision at various levels in cortical hierarchies: please see above and (Adams et al., 2013; Corlett et al., 2010; Fletcher and Frith, 2009). This failure to modulate the postsynaptic sensitivity to afferents from the PCC in the MPFC could be construed as a selective failure of attention to the attributes (or mnemonic representations) that would normally be engaged by the task. This interpretation also speaks to the role of the DMN in attention and memory (Broyd et al., 2009; Raichle, 2015).

4.3. Weaker extrinsic connectivity between networks in schizophrenia

Understanding the dialogue between the DMN and the task-positive networks (DAN and SN) may be a crucial factor in understanding the functional architecture of the brain and its abnormalities (Raichle, 2015). We identified a common pattern in the functional integration among networks across both of the groups (Fig. 3). Specifically, there were negative connections, both from the left DAN regions and the ACC of the SN, to the DMN regions. The DMN regions reciprocated positive connections to these DAN and SN regions. This pattern was also found in a recent Granger causality study during a working memory task (Pu et al., 2016) and in our DCM study during rest (Zhou et al., 2017). This pattern suggests a hierarchical relationship among these networks, and that patients with schizophrenia have the same fundamental cortical hierarchy as controls in the context of working memory.

The regions in DAN and SN typically show increased activation during external attention-demanding tasks, such as working memory tasks; and the DMN regions often show decreased activity (deactivation) during these attention-demanding tasks but show increased activation during internal orientation activities in healthy individuals. This activation in the DAN and SN – as well as this deactivation in the DMN – are robust and ubiquitous across cognitive neuroimaging studies (Toro et al., 2008). The competition relationship between the task-activation networks and the task-deactivation network has been described as anti-correlation (Fox et al., 2005), which exists both during task performance and rest (Spreng et al., 2010). The anti-correlation may reflect a fundamental functional characteristic of the brain; to effectively switch between internal and external modes of attention (Fox et al., 2005; Whitfield-Gabrieli and Ford, 2012). In this study, through the use of a generative model describing how neuronal activity gave rise to the observed BOLD responses, we were able to make inferences about the causal interactions that underlie these commonly observed anti-correlations. We found the most parsimonious model (the simplest and most accurate) was one in which the DMN was inhibited by the SN and DAN during the task. The commonly observed anti-correlations can therefore be explained by an asymmetric causal relationship between the DMN and other networks.

We also observed subtle differences in the strength of between-network connections in patients versus controls. Specifically, we found that the connectivity from the MPFC (DMN region) to the right FEF (DAN region) and the connectivity from the right FEF to the ACC (SN region) were altered in patients, although the differences were subtle. These findings suggest that directed interactions *between* networks are disrupted in schizophrenia, although these effects were small or harder

to identify than the effects *within* networks (self-connections in the DAN and the PCC to MPFC connection in the DMN).

4.4. Contextual modulatory effect in self-connections

We found an effect of WM load specifically in the DAN regions, with less self-inhibition (greater disinhibition) in the context of the 2-back relative to the 0-back condition. This task-specific effect suggests that both the patients and the controls could adjust or optimize the excitability of superficial pyramidal cells in the DAN regions, in response to context of incoming stimuli. However, we did not find strong evidence to support a difference between patients and controls in the effect of WM load. This suggests that the self-connections of these regions were modulated by the WM load to a similar extent between patients and controls. Although the modulatory effect was similar for both groups, the baseline connectivity did show a between-group effect, meaning that the same modulatory effect would have a larger or smaller consequence in each group (see supplementary materials for an example).

4.5. Clinical implications

We found that the connections that showed strong evidence for a diagnosis effect could predict the severity of clinical symptoms in schizophrenia. The connections that contributed the most to this relationship were intrinsic self-connections in the left FEF and SPL self-connection. The implicit effects on neuronal message passing and belief propagation is a recurrent theme in predictive coding (and Bayesian brain) explanations of psychotic symptoms in schizophrenia (Corlett et al., 2011; Fletcher and Frith, 2009; Powers Iii et al., 2015). In predictive coding formulations, intrinsic disinhibition corresponds to an increase in the precision afforded prediction errors at higher (association cortex) levels in the cortical hierarchy that generate top-down predictions. This has been proposed to reflect a compensatory response to a failure to attenuate sensory precision at a lower (sensory) level (Adams et al., 2013). In our case, greater intrinsic disinhibition of the dorsal attention network was positively correlated with the severity of clinical symptoms in patients with schizophrenia.

In addition, these diagnostic connections predicted impaired cognition in processing speed (digit symbol task), attention and working memory (digit forward and backward task) and executive function (verbal fluency task) in patients with schizophrenia. These findings echo the notion that working memory impairment is an important aspect of schizophrenic thought disorder (Arnsten, 2013) and potentially underlies several of the cognitive impairments observed in schizophrenia (Goldman-Rakic, 1994; Silver et al., 2003). It should be noted that these connections were identified after regressing out working memory performance as measured by the n-back task. This suggests that these cognitive and clinical measures reflect changes in effective connectivity in schizophrenia, which are associated with abnormal behavior and impaired cognition.

It should be noted that all patients were taking antipsychotic medicine at the time of scanning. Although we modeled the effect of medication within the schizophrenia group (in terms of chlorpromazine equivalents), we cannot discount a contribution of medication to the main effects of diagnostic group (because control subjects were not medicated). However, to the extent that medication varied within the patients with schizophrenia, we accounted for the implicit effects on effective connectivity within the schizophrenia cohort (which was significant in some connections – see Fig. S1). After modeling the quantitative effect of antipsychotic medicine, we still detected significant correlations between connectivity and clinical symptoms or cognitive scores. However, we note that antipsychotic medication influences estimates of functional (Lui et al., 2010), effective (Schmidt et al., 2013), and possibly structural (Shepherd et al., 2012) connectivity. Medication may serve to modulate and normalize frontoparietal connectivity in patients experiencing first-episode psychosis (Lui et al., 2010). To further determine the effect of antipsychotic medicine on effective connectivity, a longitude study on drug-naïve patients with schizophrenia may be necessary.

5. Conclusion

The main finding of the current study is that the intrinsic and extrinsic connections in three key large-scale brain networks, especially those involving prefrontal cortex, were altered in patients with schizophrenia. Previous findings of altered correlations in the BOLD time series of patients with schizophrenia may be explained by differences in asymmetric causal interactions between brain regions. Furthermore, the neuronal coupling parameters estimated using DCM were correlated with patients' clinical symptoms and impaired cognitive function. These findings provide neuroimaging evidence for the dysconnection hypothesis (and aberrant predictive coding) by emphasizing the role of excitatory–inhibitory imbalance in neural ensembles, which may lead to the dysconnectivity phenomena observed in large-scale brain networks. These findings emphasize the importance of reduced synaptic efficacy of prefrontal efferents and afferents in the pathophysiology of schizophrenia. With the advantages of PEB in analysing large-scale networks (Razi et al., 2017), future studies could extent the current study by adding subcortical and cerebellar regions (e.g. thalamic, caudate nuclei) to explore how associated subgraphs interact with each other and whether these interactions fail in patients with schizophrenia.

Acknowledgements

This work was supported by funding from the National Natural Science Foundation of China (Nos. 91132301, 91432302, and 81371476), Youth Innovation Promotion Association of Chinese Academy of Sciences (No. 2012075), and China Scholarship Council funding (No. 201504910067). KJF is funded by a Wellcome Trust Principal Research Fellowship (Ref: 088130/Z/09/Z). The authors gratefully acknowledge Huan Huang, Peifu Li and Haixia Mao in Department of Psychiatry, Renmin Hospital of Wuhan University and Jun Chen and the staff in the Radiology Department of Radiology, Renmin Hospital of Wuhan University for extensive time and effort in data acquisition.

Appendix A. Supplementary data

Supplementary data to this article can be found online at https://doi.org/10.1016/j.nicl.2017.12.006.

References

Abi-Saab, W.M., D'Souza, D.C., Moghaddam, B., Krystal, J.H., 1998. The NMDA antagonist model for schizophrenia: promise and pitfalls. Pharmacopsychiatry 31 (Suppl. 2), 104–109. http://dx.doi.org/10.1055/s-2007-979354.

Adams, R.A., Stephan, K.E., Brown, H.R., Frith, C.D., Friston, K.J., 2013. The computational anatomy of psychosis. Front. Psych. 4, 47. http://dx.doi.org/10.3389/fpsyt.2013.00047.

Andreasen, N.C., Paradiso, S., O'Leary, D.S., 1998. "Cognitive dysmetria" as an integrative theory of schizophrenia: a dysfunction in cortical-subcortical-cerebellar circuitry? Schizophr. Bull. 24, 203–218. http://www.ncbi.nlm.nih.gov/pubmed/9613621.

Andrews-Hanna, J.R., Reidler, J.S., Huang, C., Buckner, R.L., 2010. Evidence for the default network's role in spontaneous cognition. J. Neurophysiol. 104, 322–335. http://dx.doi.org/10.1152/jn.00830.2009.

Anticevic, A., Repovs, G., Barch, D.M., 2013. Working memory encoding and maintenance deficits in schizophrenia: neural evidence for activation and deactivation abnormalities. Schizophr. Bull. 39, 168–178. http://dx.doi.org/10.1093/schbul/sbr107.

Arnsten, A.F., 2013. The neurobiology of thought: the groundbreaking discoveries of Patricia Goldman-Rakic 1937–2003. Cereb. Cortex 23, 2269–2281. http://dx.doi.org/10.1093/cercor/bht195.

Bastos, A.M., Usrey, W.M., Adams, R.A., Mangun, G.R., Fries, P., Friston, K.J., 2012. Canonical microcircuits for predictive coding. Neuron 76, 695–711. http://dx.doi.org/10.1016/j.neuron.2012.10.038.

Bastos-Leite, A.J., Ridgway, G.R., Silveira, C., Norton, A., Reis, S., Friston, K.J., 2015. Dysconnectivity within the default mode in first-episode schizophrenia: a stochastic

dynamic causal modeling study with functional magnetic resonance imaging. Schizophr. Bull. 41, 144–153. http://dx.doi.org/10.1093/schbul/sbu080.
Behzadi, Y., Restom, K., Liau, J., Liu, T.T., 2007. A component based noise correction method (CompCor) for BOLD and perfusion based fMRI. NeuroImage 37, 90–101. http://dx.doi.org/10.1016/j.neuroimage.2007.04.042.
Bora, E., Yucel, M., Pantelis, C., 2010. Cognitive impairment in schizophrenia and affective psychoses: implications for DSM-V criteria and beyond. Schizophr. Bull. 36, 36–42. http://dx.doi.org/10.1093/schbul/sbp094.
Braun, U., Schafer, A., Bassett, D.S., Rausch, F., Schweiger, J.I., Bilek, E., Erk, S., Romanczuk-Seiferth, N., Grimm, O., Geiger, L.S., Haddad, L., Otto, K., Mohnke, S., Heinz, A., Zink, M., Walter, H., Schwarz, E., Meyer-Lindenberg, A., Tost, H., 2016. Dynamic brain network reconfiguration as a potential schizophrenia genetic risk mechanism modulated by NMDA receptor function. Proc. Natl. Acad. Sci. U. S. A. 113, 12568–12573. http://dx.doi.org/10.1073/pnas.1608819113.
Breakspear, M., 2004. "Dynamic" connectivity in neural systems: theoretical and empirical considerations. Neuroinformatics 2, 205–226. http://dx.doi.org/10.1385/NI:2:2:205.
Broyd, S.J., Demanuele, C., Debener, S., Helps, S.K., James, C.J., Sonuga-Barke, E.J., 2009. Default-mode brain dysfunction in mental disorders: a systematic review. Neurosci. Biobehav. Rev. 33, 279–296. http://dx.doi.org/10.1016/j.neubiorev.2008.09.002.
Buckner, R.L., Andrews-Hanna, J.R., Schacter, D.L., 2008. The brain's default network: anatomy, function, and relevance to disease. Ann. N. Y. Acad. Sci. 1124, 1–38. http://dx.doi.org/10.1196/annals.1440.011.
Bullmore, E.T., Frangou, S., Murray, R.M., 1997. The dysplastic net hypothesis: an integration of developmental and dysconnectivity theories of schizophrenia. Schizophr. Res. 28, 143–156. http://www.ncbi.nlm.nih.gov/entrez/query.fcgi?cmd=Retrieve&db=PubMed&dopt=Citation&list_uids=9468349.
Carlen, M., Meletis, K., Siegle, J.H., Cardin, J.A., Futai, K., Vierling-Claassen, D., Ruhlmann, C., Jones, S.R., Deisseroth, K., Sheng, M., Moore, C.I., Tsai, L.H., 2012. A critical role for NMDA receptors in parvalbumin interneurons for gamma rhythm induction and behavior. Mol. Psychiatry 17, 537–548. http://dx.doi.org/10.1038/mp.2011.31.
Chu, C., Fan, L., Eickhoff, C.R., Liu, Y., Yang, Y., Eickhoff, S.B., Jiang, T., 2015. Coactivation Probability Estimation (CoPE): an approach for modeling functional coactivation architecture based on neuroimaging coordinates. NeuroImage 117, 397–407. http://dx.doi.org/10.1016/j.neuroimage.2015.05.069.
Clark, A., 2013. The many faces of precision (replies to commentaries on "Whatever next? Neural prediction, situated agents, and the future of cognitive science"). Front. Psychol. 4, 270. http://dx.doi.org/10.3389/fpsyg.2013.00270.
Corbetta, M., Shulman, G.L., 2002. Control of goal-directed and stimulus-driven attention in the brain. Nat. Rev. Neurosci. 3, 201–215. http://dx.doi.org/10.1038/nrn755.
Corlett, P.R., Taylor, J.R., Wang, X.J., Fletcher, P.C., Krystal, J.H., 2010. Toward a neurobiology of delusions. Prog. Neurobiol. 92, 345–369. http://dx.doi.org/10.1016/j.pneurobio.2010.06.007.
Corlett, P.R., Honey, G.D., Krystal, J.H., Fletcher, P.C., 2011. Glutamatergic model psychoses: prediction error, learning, and inference. Neuropsychopharmacology 36, 294–315. http://dx.doi.org/10.1038/npp.2010.163.
Coyle, J.T., Tsai, G., Goff, D., 2003. Converging evidence of NMDA receptor hypofunction in the pathophysiology of schizophrenia. Ann. N. Y. Acad. Sci. 1003, 318–327. https://www.ncbi.nlm.nih.gov/pubmed/14684455.
Crossley, N.A., Mechelli, A., Fusar-Poli, P., Broome, M.R., Matthiasson, P., Johns, L.C., Bramon, E., Valmaggia, L., Williams, S.C., McGuire, P.K., 2009. Superior temporal lobe dysfunction and frontotemporal dysconnectivity in subjects at risk of psychosis and in first-episode psychosis. Hum. Brain Mapp. 30, 4129–4137. http://dx.doi.org/10.1002/hbm.20834.
Deserno, L., Sterzer, P., Wustenberg, T., Heinz, A., Schlagenhauf, F., 2012. Reduced prefrontal-parietal effective connectivity and working memory deficits in schizophrenia. J. Neurosci. 32, 12–20. http://dx.doi.org/10.1523/JNEUROSCI.3405-11.2012.
Dosenbach, N.U., Fair, D.A., Miezin, F.M., Cohen, A.L., Wenger, K.K., Dosenbach, R.A., Fox, M.D., Snyder, A.Z., Vincent, J.L., Raichle, M.E., Schlaggar, B.L., Petersen, S.E., 2007. Distinct brain networks for adaptive and stable task control in humans. Proc. Natl. Acad. Sci. U. S. A. 104, 11073–11078. http://dx.doi.org/10.1073/pnas.0704320104.
Fletcher, P.C., Frith, C.D., 2009. Perceiving is believing: a Bayesian approach to explaining the positive symptoms of schizophrenia. Nat. Rev. Neurosci. 10, 48–58.
Forbes, N.F., Carrick, L.A., McIntosh, A.M., Lawrie, S.M., 2009. Working memory in schizophrenia: a meta-analysis. Psychol. Med. 39, 889–905. http://dx.doi.org/10.1017/S0033291708004558.
Fornito, A., Bullmore, E.T., 2015. Reconciling abnormalities of brain network structure and function in schizophrenia. Curr. Opin. Neurobiol. 30, 44–50. http://dx.doi.org/10.1016/j.conb.2014.08.006.
Fox, M.D., Corbetta, M., Snyder, A.Z., Vincent, J.L., Raichle, M.E., 2006. Spontaneous neuronal activity distinguishes human dorsal and ventral attention systems. Proc. Natl. Acad. Sci. U. S. A. 103, 10046–10051. http://dx.doi.org/10.1073/pnas.0604187103.
Fox, M.D., Snyder, A.Z., Vincent, J.L., Corbetta, M., Van Essen, D.C., Raichle, M.E., 2005. The human brain is intrinsically organized into dynamic, anticorrelated functional networks. Proc. Natl. Acad. Sci. U. S. A. 102, 9673–9678. http://dx.doi.org/10.1073/pnas.0504136102.
Friston, K., Brown, H.R., Siemerkus, J., Stephan, K.E., 2016. The dysconnection hypothesis (2016). Schizophr. Res. 176, 83–94. http://dx.doi.org/10.1016/j.schres.2016.07.014.
Friston, K., Moran, R., Seth, A.K., 2013. Analysing connectivity with Granger causality and dynamic causal modelling. Curr. Opin. Neurobiol. 23, 172–178. http://dx.doi.org/10.1016/j.conb.2012.11.010.
Friston, K.J., 2011. Functional and effective connectivity: a review. Brain Connect. 1, 13–36. http://dx.doi.org/10.1089/brain.2011.0008.
Friston, K.J., Frith, C.D., 1995. Schizophrenia: a disconnection syndrome? Clin. Neurosci. 3, 89–97. http://www.ncbi.nlm.nih.gov/entrez/query.fcgi?cmd=Retrieve&db=PubMed&dopt=Citation&list_uids=7583624.
Friston, K.J., Frith, C.D., Liddle, P.F., Frackowiak, R.S., 1993. Functional connectivity: the principal-component analysis of large (PET) data sets. J. Cereb. Blood Flow Metab. 13, 5–14.
Friston, K.J., Harrison, L., Penny, W., 2003. Dynamic causal modelling. NeuroImage 19, 1273–1302. https://www.ncbi.nlm.nih.gov/pubmed/12948688.
Friston, K.J., Litvak, V., Oswal, A., Razi, A., Stephan, K.E., van Wijk, B.C., Ziegler, G., Zeidman, P., 2016. Bayesian model reduction and empirical Bayes for group (DCM) studies. NeuroImage 128, 413–431. http://dx.doi.org/10.1016/j.neuroimage.2015.11.015.
Friston, K.J., Stephan, K.E., Montague, R., Dolan, R.J., 2014. Computational psychiatry: the brain as a phantastic organ. Lancet Psychiatry 1, 148–158. http://dx.doi.org/10.1016/S2215-0366(14)70275-5.
Gilmour, G., Dix, S., Fellini, L., Gastambide, F., Plath, N., Steckler, T., Talpos, J., Tricklebank, M., 2012. NMDA receptors, cognition and schizophrenia–testing the validity of the NMDA receptor hypofunction hypothesis. Neuropharmacology 62, 1401–1412. http://dx.doi.org/10.1016/j.neuropharm.2011.03.015.
Goldman-Rakic, P.S., 1994. Working memory dysfunction in schizophrenia. J. Neuropsychiatr. Clin. Neurosci. 6, 348–357. http://www.ncbi.nlm.nih.gov/entrez/query.fcgi?cmd=Retrieve&db=PubMed&dopt=Citation&list_uids=7841806.
Haatveit, B., Jensen, J., Alnaes, D., Kaufmann, T., Brandt, C.L., Thoresen, C., Andreassen, O.A., Melle, I., Ueland, T., Westlye, L.T., 2016. Reduced load-dependent default mode network deactivation across executive tasks in schizophrenia spectrum disorders. Neuroimage Clin. 12, 389–396. http://dx.doi.org/10.1016/j.nicl.2016.08.012.
Jiang, T., Zhou, Y., Liu, B., Liu, Y., Song, M., 2013. Brainnetome-wide association studies in schizophrenia: the advances and future. Neurosci. Biobehav. Rev. 37, 2818–2835. http://dx.doi.org/10.1016/j.neubiorev.2013.10.004.
Kim, M.A., Tura, E., Potkin, S.G., Fallon, J.H., Manoach, D.S., Calhoun, V.D., Fbirn, Turner, J.A., 2010. Working memory circuitry in schizophrenia shows widespread cortical inefficiency and compensation. Schizophr. Res. 117, 42–51. http://dx.doi.org/10.1016/j.schres.2009.12.014.
Knowles, E.E., David, A.S., Reichenberg, A., 2010. Processing speed deficits in schizophrenia: reexamining the evidence. Am. J. Psychiatry 167, 828–835. http://dx.doi.org/10.1176/appi.ajp.2010.09070937.
Kyriakopoulos, M., Dima, D., Roiser, J.P., Corrigall, R., Barker, G.J., Frangou, S., 2012. Abnormal functional activation and connectivity in the working memory network in early-onset schizophrenia. J. Am. Acad. Child Adolesc. Psychiatry 51, 911–920. e912. https://doi.org/10.1016/j.jaac.2012.06.020.
Lee, J., Park, S., 2005. Working memory impairments in schizophrenia: a meta-analysis. J. Abnorm. Psychol. 114, 599–611. http://dx.doi.org/10.1037/0021-843X.114.4.599.
Lewis, D.A., Curley, A.A., Glausier, J.R., Volk, D.W., 2012. Cortical parvalbumin interneurons and cognitive dysfunction in schizophrenia. Trends Neurosci. 35, 57–67. http://dx.doi.org/10.1016/j.tins.2011.10.004.
Lui, S., Li, T., Deng, W., Jiang, L., Wu, Q., Tang, H., Yue, Q., Huang, X., Chan, R.C., Collier, D.A., Meda, S.A., Pearlson, G., Mechelli, A., Sweeney, J.A., Gong, Q., 2010. Short-term effects of antipsychotic treatment on cerebral function in drug-naive first-episode schizophrenia revealed by "resting state" functional magnetic resonance imaging. Arch. Gen. Psychiatry 67, 783–792. http://dx.doi.org/10.1001/archgenpsychiatry.2010.84.
Menon, V., Uddin, L.Q., 2010. Saliency, switching, attention and control: a network model of insula function. Brain Struct. Funct. 214, 655–667. http://dx.doi.org/10.1007/s00429-010-0262-0.
Monaco, S.A., Gulchina, Y., Gao, W.J., 2015. NR2B subunit in the prefrontal cortex: a double-edged sword for working memory function and psychiatric disorders. Neurosci. Biobehav. Rev. 56, 127–138. http://dx.doi.org/10.1016/j.neubiorev.2015.06.022.
Murray, J.D., Anticevic, A., Gancsos, M., Ichinose, M., Corlett, P.R., Krystal, J.H., Wang, X.J., 2014. Linking microcircuit dysfunction to cognitive impairment: effects of disinhibition associated with schizophrenia in a cortical working memory model. Cereb. Cortex 24, 859–872. http://dx.doi.org/10.1093/cercor/bhs370.
Nielsen, J.D., Madsen, K.H., Wang, Z., Liu, Z., Friston, K.J., Zhou, Y., 2017. Working memory modulation of frontoparietal network connectivity in first-episode schizophrenia. Cereb. Cortex 1–10. http://dx.doi.org/10.1093/cercor/bhx050.
Olney, J.W., Newcomer, J.W., Farber, N.B., 1999. NMDA receptor hypofunction model of schizophrenia. J. Psychiatr. Res. 33, 523–533. https://www.ncbi.nlm.nih.gov/pubmed/10628529.
Owen, A.M., McMillan, K.M., Laird, A.R., Bullmore, E., 2005. N-back working memory paradigm: a meta-analysis of normative functional neuroimaging studies. Hum. Brain Mapp. 25, 46–59. http://dx.doi.org/10.1002/hbm.20131.
Pettersson-Yeo, W., Allen, P., Benetti, S., McGuire, P., Mechelli, A., 2011. Dysconnectivity in schizophrenia: where are we now? Neurosci. Biobehav. Rev. 35, 1110–1124. http://dx.doi.org/10.1016/j.neubiorev.2010.11.004.
Phillips, W.A., Silverstein, S.M., 2003. Convergence of biological and psychological perspectives on cognitive coordination in schizophrenia. Behav. Brain Sci. 26, 65–82 discussion 82–137. (https://www.ncbi.nlm.nih.gov/pubmed/14598440).
Piskulic, D., Olver, J.S., Norman, T.R., Maruff, P., 2007. Behavioural studies of spatial working memory dysfunction in schizophrenia: a quantitative literature review. Psychiatry Res. 150, 111–121. http://dx.doi.org/10.1016/j.psychres.2006.03.018.
Power, J.D., Barnes, K.A., Snyder, A.Z., Schlaggar, B.L., Petersen, S.E., 2012. Spurious but systematic correlations in functional connectivity MRI networks arise from subject

motion. NeuroImage 59, 2142–2154. http://dx.doi.org/10.1016/j.neuroimage.2011.10.018.
Powers Iii, A.R., Gancsos, M.G., Finn, E.S., Morgan, P.T., Corlett, P.R., 2015. Ketamine-induced hallucinations. Psychopathology 48, 376–385. http://dx.doi.org/10.1159/000438675.
Pu, W., Luo, Q., Palaniyappan, L., Xue, Z., Yao, S., Feng, J., Liu, Z., 2016. Failed cooperative, but not competitive, interaction between large-scale brain networks impairs working memory in schizophrenia. Psychol. Med. 46, 1211–1224. http://dx.doi.org/10.1017/S0033291715002755.
Raichle, M.E., 2015. The Brain's default mode network. Annu. Rev. Neurosci. 38, 433–447. http://dx.doi.org/10.1146/annurev-neuro-071013-014030.
Ranlund, S., Adams, R.A., Diez, A., Constante, M., Dutt, A., Hall, M.H., Maestro Carbayo, A., McDonald, C., Petrella, S., Schulze, K., Shaikh, M., Walshe, M., Friston, K., Pinotsis, D., Bramon, E., 2016. Impaired prefrontal synaptic gain in people with psychosis and their relatives during the mismatch negativity. Hum. Brain Mapp. 37, 351–365. http://dx.doi.org/10.1002/hbm.23035.
Razi, A., Seghier, M.L., Zhou, Y., McColgan, P., Zeidman, P., Park, H.-J., Sporns, O., Rees, G., Friston, K.J., 2017. Large-scale DCMs for resting-state fMRI. Network Neuroscience 1 (3), 222–241. http://dx.doi.org/10.1162/netn_a_00015.
Rottschy, C., Langner, R., Dogan, I., Reetz, K., Laird, A.R., Schulz, J.B., Fox, P.T., Eickhoff, S.B., 2012. Modelling neural correlates of working memory: a coordinate-based meta-analysis. NeuroImage 60, 830–846. http://dx.doi.org/10.1016/j.neuroimage.2011.11.050.
Salomon, R., Bleich-Cohen, M., Hahamy-Dubossarsky, A., Dinstien, I., Weizman, R., Poyurovsky, M., Kupchik, M., Kotler, M., Hendler, T., Malach, R., 2011. Global functional connectivity deficits in schizophrenia depend on behavioral state. J. Neurosci. 31, 12972–12981. http://dx.doi.org/10.1523/JNEUROSCI.2987-11.2011.
Satterthwaite, T.D., Wolf, D.H., Loughead, J., Ruparel, K., Elliott, M.A., Hakonarson, H., Gur, R.C., Gur, R.E., 2012. Impact of in-scanner head motion on multiple measures of functional connectivity: relevance for studies of neurodevelopment in youth. NeuroImage 60, 623–632. http://dx.doi.org/10.1016/j.neuroimage.2011.12.063.
Schmidt, A., Smieskova, R., Aston, J., Simon, A., Allen, P., Fusar-Poli, P., McGuire, P.K., Riecher-Rossler, A., Stephan, K.E., Borgwardt, S., 2013. Brain connectivity abnormalities predating the onset of psychosis: correlation with the effect of medication. JAMA Psychiat. 70, 903–912. http://dx.doi.org/10.1001/jamapsychiatry.2013.117.
Schmidt, A., Smieskova, R., Simon, A., Allen, P., Fusar-Poli, P., McGuire, P.K., Bendfeldt, K., Aston, J., Lang, U.E., Walter, M., Radue, E.W., Riecher-Rossler, A., Borgwardt, S.J., 2014. Abnormal effective connectivity and psychopathological symptoms in the psychosis high-risk state. J. Psychiatry Neurosci. 39, 239–248. http://www.ncbi.nlm.nih.gov/pubmed/24506946.
Seeley, W.W., Menon, V., Schatzberg, A.F., Keller, J., Glover, G.H., Kenna, H., Reiss, A.L., Greicius, M.D., 2007. Dissociable intrinsic connectivity networks for salience processing and executive control. J. Neurosci. 27, 2349–2356. http://dx.doi.org/10.1523/JNEUROSCI.5587-06.2007.
Shepherd, A.M., Laurens, K.R., Matheson, S.L., Carr, V.J., Green, M.J., 2012. Systematic meta-review and quality assessment of the structural brain alterations in schizophrenia. Neurosci. Biobehav. Rev. 36, 1342–1356. http://dx.doi.org/10.1016/j.neubiorev.2011.12.015.
Shirer, W.R., Ryali, S., Rykhlevskaia, E., Menon, V., Greicius, M.D., 2012. Decoding subject-driven cognitive states with whole-brain connectivity patterns. Cereb. Cortex 22, 158–165. http://dx.doi.org/10.1093/cercor/bhr099.
Silver, H., Feldman, P., Bilker, W., Gur, R.C., 2003. Working memory deficit as a core neuropsychological dysfunction in schizophrenia. Am. J. Psychiatr. 160, 1809–1816.
Spreng, R.N., Stevens, W.D., Chamberlain, J.P., Gilmore, A.W., Schacter, D.L., 2010. Default network activity, coupled with the frontoparietal control network, supports goal-directed cognition. NeuroImage 53, 303–317. http://dx.doi.org/10.1016/j.neuroimage.2010.06.016.
Stanislaw, H., Todorov, N., 1999. Calculation of signal detection theory measures. Behav. Res. Methods Instrum. Comput. 31, 137–149. http://www.ncbi.nlm.nih.gov/pubmed/10495845.
Stephan, K.E., Baldeweg, T., Friston, K.J., 2006. Synaptic plasticity and dysconnection in schizophrenia. Biol. Psychiatry 59, 929–939. http://dx.doi.org/10.1016/j.biopsych.2005.10.005.
Sui, J., Adali, T., Yu, Q., Chen, J., Calhoun, V.D., 2012. A review of multivariate methods for multimodal fusion of brain imaging data. J. Neurosci. Methods 204, 68–81. http://dx.doi.org/10.1016/j.jneumeth.2011.10.031.
Toro, R., Fox, P.T., Paus, T., 2008. Functional coactivation map of the human brain. Cereb. Cortex 18, 2553–2559. http://dx.doi.org/10.1093/cercor/bhn014.
Uhlhaas, P.J., Singer, W., 2012. Neuronal dynamics and neuropsychiatric disorders: toward a translational paradigm for dysfunctional large-scale networks. Neuron 75, 963–980. http://dx.doi.org/10.1016/j.neuron.2012.09.004.
Van Dijk, K.R., Sabuncu, M.R., Buckner, R.L., 2012. The influence of head motion on intrinsic functional connectivity MRI. NeuroImage 59, 431–438. http://dx.doi.org/10.1016/j.neuroimage.2011.07.044.
Weinberger, D.R., 1993. A connectionist approach to the prefrontal cortex. J. Neuropsychiatr. Clin. Neurosci. 5, 241–253. http://dx.doi.org/10.1176/jnp.5.3.241.
Whitfield-Gabrieli, S., Ford, J.M., 2012. Default mode network activity and connectivity in psychopathology. Annu. Rev. Clin. Psychol. 8, 49–76. http://dx.doi.org/10.1146/annurev-clinpsy-032511-143049.
Whitfield-Gabrieli, S., Thermenos, H.W., Milanovic, S., Tsuang, M.T., Faraone, S.V., McCarley, R.W., Shenton, M.E., Green, A.I., Nieto-Castanon, A., LaViolette, P., Wojcik, J., Gabrieli, J.D., Seidman, L.J., 2009. Hyperactivity and hyperconnectivity of the default network in schizophrenia and in first-degree relatives of persons with schizophrenia. Proc. Natl. Acad. Sci. U. S. A. 106, 1279–1284. http://dx.doi.org/10.1073/pnas.0809141106.
Wu, G., Wang, Y., Mwansisya, T.E., Pu, W., Zhang, H., Liu, C., Yang, Q., Chen, E.Y., Xue, Z., Liu, Z., Shan, B., 2014. Effective connectivity of the posterior cingulate and medial prefrontal cortices relates to working memory impairment in schizophrenic and bipolar patients. Schizophr. Res. 158, 85–90. http://dx.doi.org/10.1016/j.schres.2014.06.033.
Wu, S., Wang, H., Chen, C., Zou, J., Huang, H., Li, P., Zhao, Y., Xu, Q., Zhang, L., Wang, H., Pandit, S., Dahal, S., Chen, J., Zhou, Y., Jiang, T., Wang, G., 2017. Task performance modulates functional connectivity involving the dorsolateral prefrontal cortex in patients with schizophrenia. Front. Psychol. 8, 56. http://dx.doi.org/10.3389/fpsyg.2017.00056.
Zhang, H., Wei, X., Tao, H., Mwansisya, T.E., Pu, W., He, Z., Hu, A., Xu, L., Liu, Z., Shan, B., Xue, Z., 2013. Opposite effective connectivity in the posterior cingulate and medial prefrontal cortex between first-episode schizophrenic patients with suicide risk and healthy controls. PLoS One 8, e63477. http://dx.doi.org/10.1371/journal.pone.0063477.
Zhou, Y., Friston, K.J., Zeidman, P., Chen, J., Li, S., Razi, A., 2017. The Hierarchical Organization of the Default, Dorsal Attention and Salience Networks in Adolescents and Young Adults. Cereb. Cortex 1–12. http://dx.doi.org/10.1093/cercor/bhx307.